EXTERNAL MUON IDENTIFIER DEVELOPMENT:

HALF METER PROPORTIONAL CHAMBER TEST RESULTS

Sherwood Parker, University of Hawaii and

Ronald Jones, Lawrence Berkeley Laboratory

A. Introduction

A half scale multi-wire proportional chamber has been built to

determine the optimum gap and to test several proposed features of the

1 meter chambers that will form the muon-identifier detector elements.

The chambers and their readout system are designed to be simple and

inexpensive. The main features are:

1. Three coordinate readout--X, Y (90°), and U (63° now, to be 45° in

the 1 m chambers)--using only one wire plane.

2. A copper strip--plastic laminate that serves as a gas barrier, cathode,

and conveyer of induced signals for the Y and U coordinates.

3. An electromagnetic delay line readout[1] that also provides a prompt

timing pulse.

4. A wire-to-wire separation (5 mm) sufficiently large to prevent

electrostatic instability[2] without the need for supporting structures.

The system resolution will be limited, in any event, by the delay line

electronics cycle time. In principle, however, resolution in the

direction parallel to the wire plane can be made much finer than the

wire spacing.[1]

5. The 1/2 m chamber gap was made adjustable through the use of spacer

frames.

6. The 1 m chamber has been designed to minimize machining. Only sawing,

drilling, gluing, and soldering will be needed in its construction.

7. The cathode planes are kept flat with a light-weight, non-conducting

sandwich material. The 1/2 m chamber uses Mylar bonded to polyurethane foam, while the 1 m chamber will use Mylar bonded to a paper honeycomb material.

B. The Main Test Results are:

1. A plastic - copper laminate with the copper etched to make conductive strips makes a satisfactory cathode and gas barrier. No charging or shielding problems were observed. A number of subtle effects were found which played a significant role in the 1 m chamber design.

2. The maximum gain for various gasses and gaps was determined. We understand in general, what sets the limits. This information was used in determining the optimum gap thickness.

3. Satisfactory delay line and prompt outputs have been achieved. RMS resolution should be of the order of ± several mm. (The electronics cycle time of 40 ns will broaden this somewhat.)

4. The amplified output from the delay line will easily drive a cable long enough to make the run between neutrino Labs B and A, eliminating the need for a trailer,   electronic racks in a high magnetic field, expensive 66 twisted - pair cable (more $ than coax), and many cold walks in the Illinois snow. We will also be able to monitor the the raw signals directly. Tests for electromagnetic interference, however, remain to be performed.

5. The chamber gave no spurious signals when subjected to a vibration test (hit the table with a hammer). Legitimate signals also did not change in pulse height.

6. The efficiency for perpendicular, changed tracks was measured to be $100 \pm \frac{1}{2}$ %.

7. The two-pulse resolution depends on the relative size of the pulses and ranges, typically, from 2.5 to 6.5 cm.

8. The following 1/2 m chamber work remains to be done:

   a. Feed the discriminator outputs to the digitizers and computer.

   b. Test the chamber in a high magnetic field.

   c. Complete a life test (partly done already with the many hours of running with hot ^{90}Sr, ^{55}Fe, and ^{109}Cd sources).

C. Details and Additional Results:

1. Construction

Figure 1 shows one of the cathode planes. A 1/2 m delay line is shown on the coupling pad region. Figure 2 shows the assembled 1/2 m chamber with the delay lines, preamplifiers, and fiducial driver. Figures 3 to 6 show the 1 m chamber design. The basic idea is to avoid machining by building the chamber of strips sawed from uniform, preground sheet of G10 fiberglass which is readily available for not too much more than the basic material cost. A 0.5 m test strip was sawed with a carborundum table saw in less than one minute. The finish was smooth, the surface was free of visible carbonization, and the width was uniform to $\pm$.04 mm.

The cathode planes are made from Kapton bonded to 1.4 mil Cu. The Cu was etched and plated with a thin Au coat to provide the proper strip pattern for the Y (90°) and U (63°) planes.

The 1 m chamber will have to use Mylar (.005 in.)--due to our inability to find Kapton--Cu in sufficient widths. The electrical and mechanical properties of Mylar are just about as good as those of Kapton but it tends to melt when you solder to the Cu if you are not fast. However, we have greatly reduced the number of solder joints needed (from
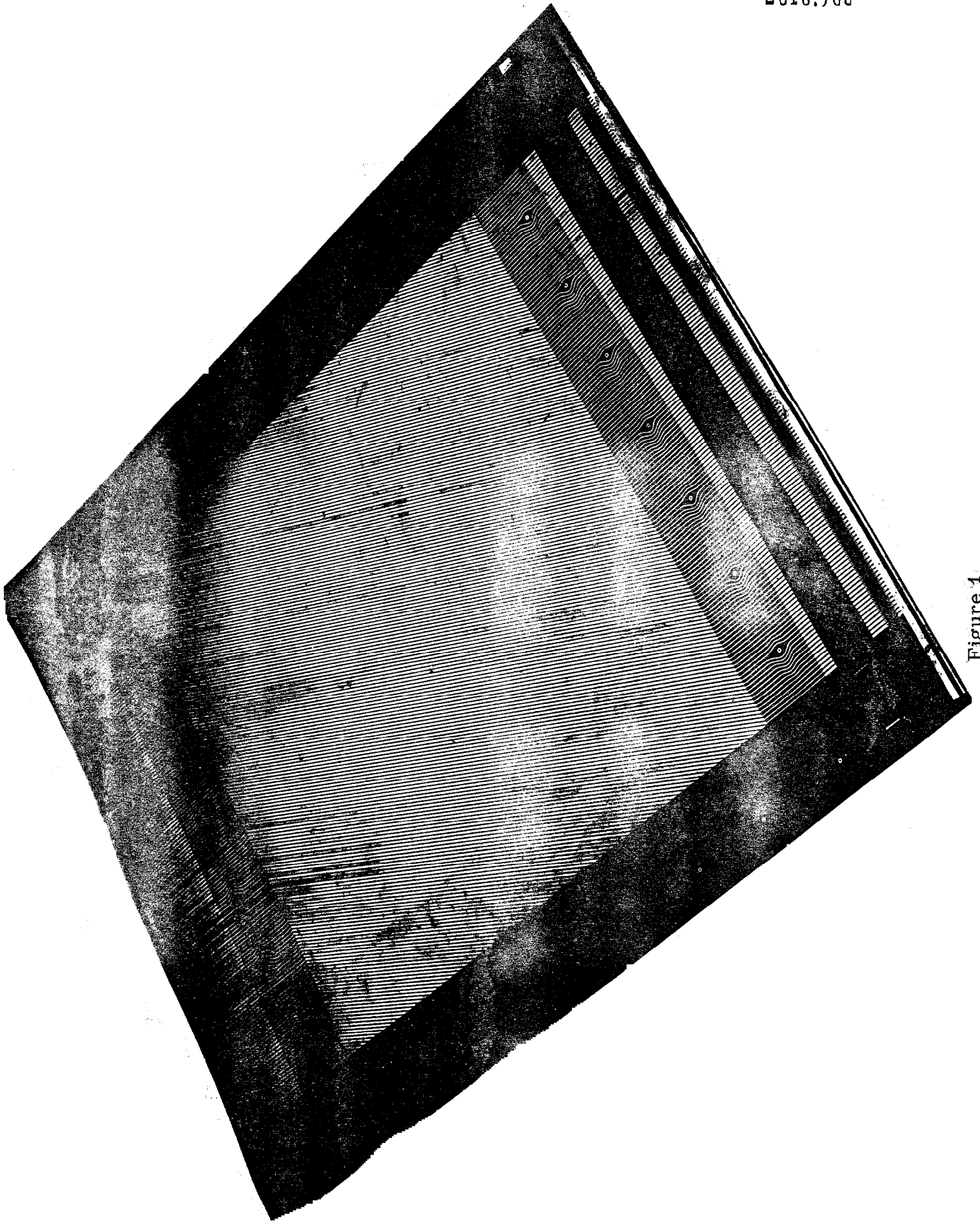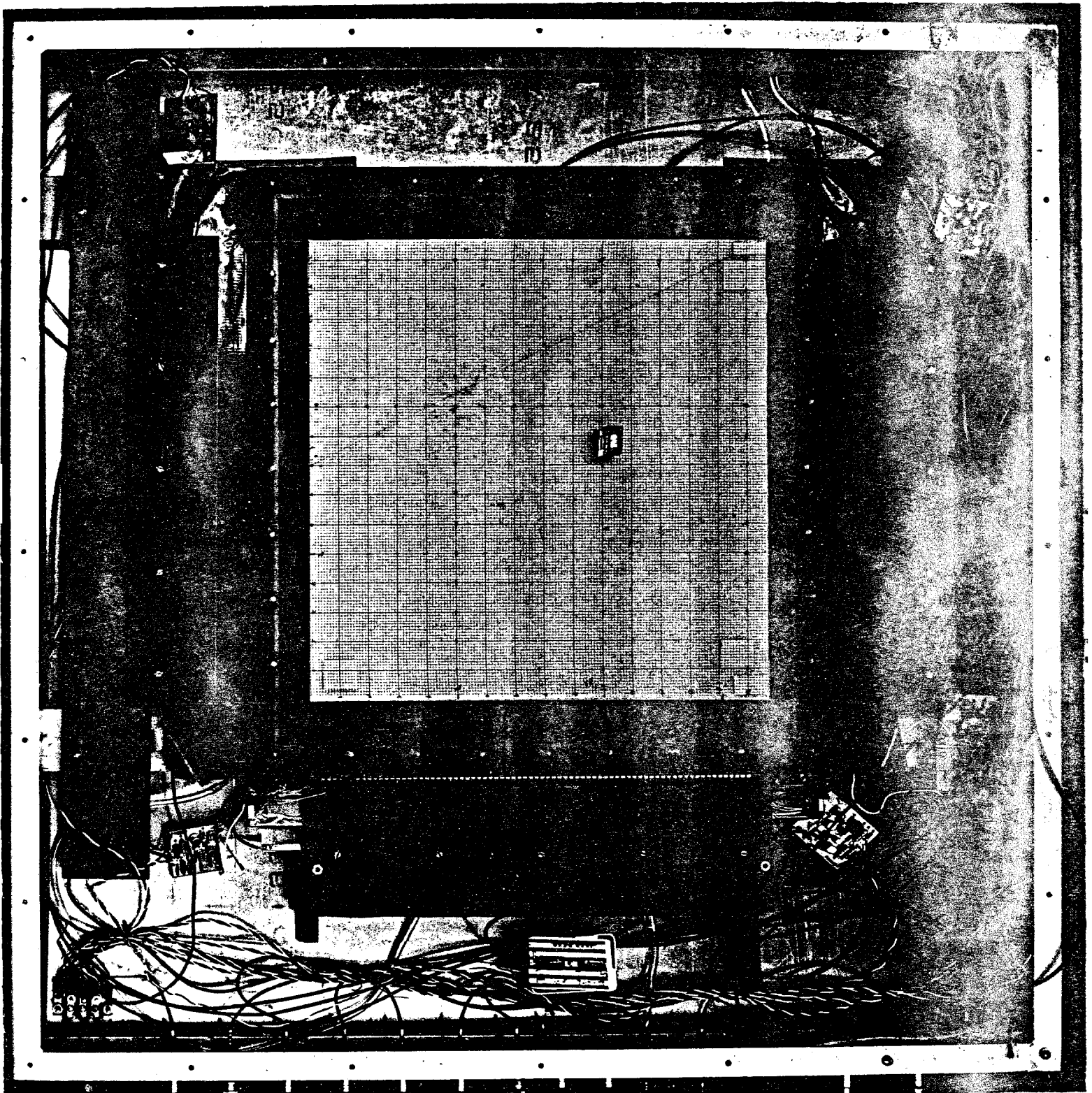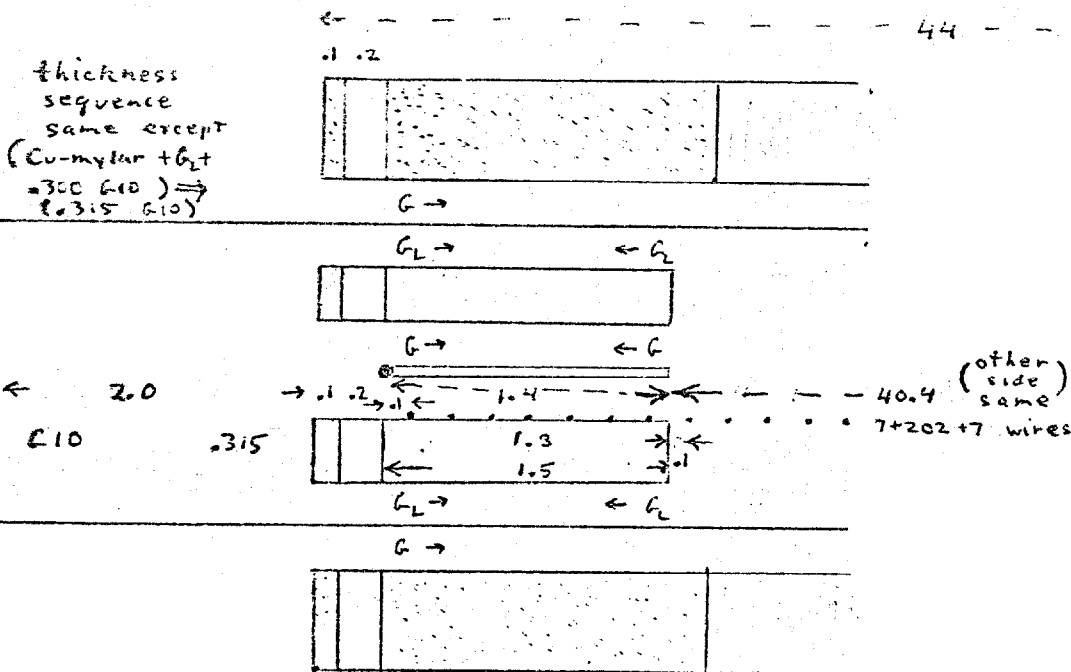
Figure 1

Figure 2

— — — — — — — 44 — — — —

.1 .2"

mylar skin .015

core .5

mylar skin .015

Cu-mylar .005
.007

G 10 .270 ← — — 40.4 — — →

O ring, G10 .005
.040

Cu-mylar .1 .2 ← .6 →   .8 →   ← .8   .6 → .2 .1

(extends out 1.6) .007 .008

G 10 .300   .315

Cu-mylar .005
.007

mylar skin .005
.015

core .5

mylar skin .015

1.724

2 nuts (.132) 1.488

↑ 10-32 clearance

← — — — — — — 44 — —

.1 .2

thickness
sequence
same except
(Cu-mylar + G₂ +
.300 G10) →
(.315 G10)

G →

G_L →   ← G₂

G →   ← G

← 2.0 → .1 .2 .1 ← 1.4 — — → ← — 40.4   (other side same)
                                         7 + 202 + 7 wires

G10 .315

1.3

1.5

G_L →   ← G₂

G →

Figure 3

Notes:
1. all dimensions in inches
2. wire dia. 0.0008
3. wire spacing 0.2
4. material

Hexcel frame
Nomex core HRH-10
G10

● 1/16" O ring (dia.)
solder
epoxy bead (or
indicated by
letters G→←G,
G₂→←G₂ (leak tight))

5. wire epoxy bead ~.03-.04
thick; other epoxy
joints assumed to be
~.005 thick (±.002)
6. G10 thickness tolerance ±

Bottom G10 Frame

TM-359
2610.900

.2 3.8 ←

44
10 x 3.6

→ 3.8 .2

.2

3.8

.2

3.8

1.8 x 44 x .315

10 x 3.6

← 1.8 x 40.4 x .315

fine wire
direction

1.8 x 40.4 x .315 →

10 x 3.6

44

1.8 x 44 x .300

3.8

.2

3.8

.2

.2 3.8

10 x 3.6

3.8 .2

(A)
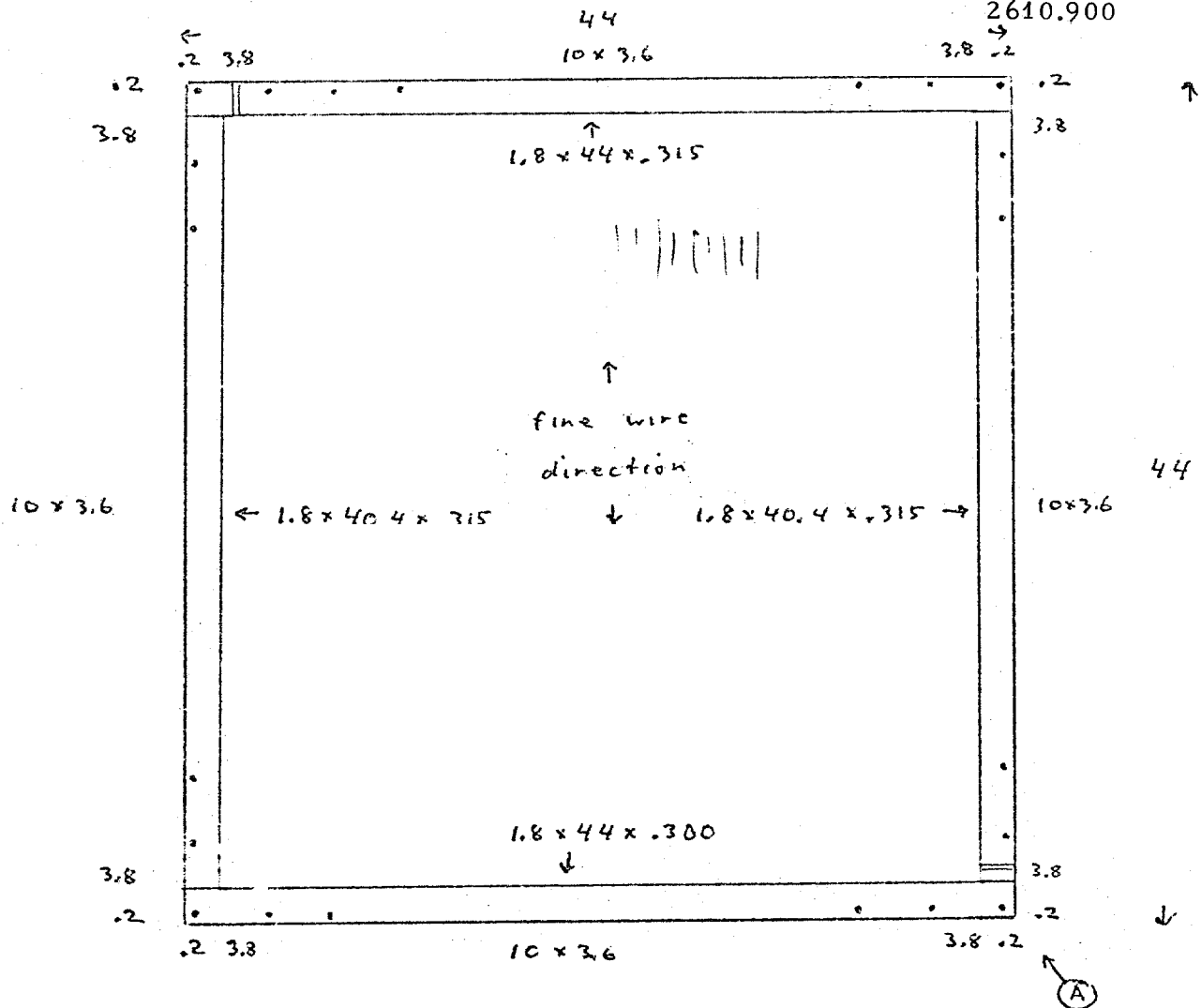
1. holes are 0.2 dia

2. distances shown between centers except 0.2 between
   center and edge

3. 3D view of corner (A)

← 1.8

→ ↕ .315

G-10

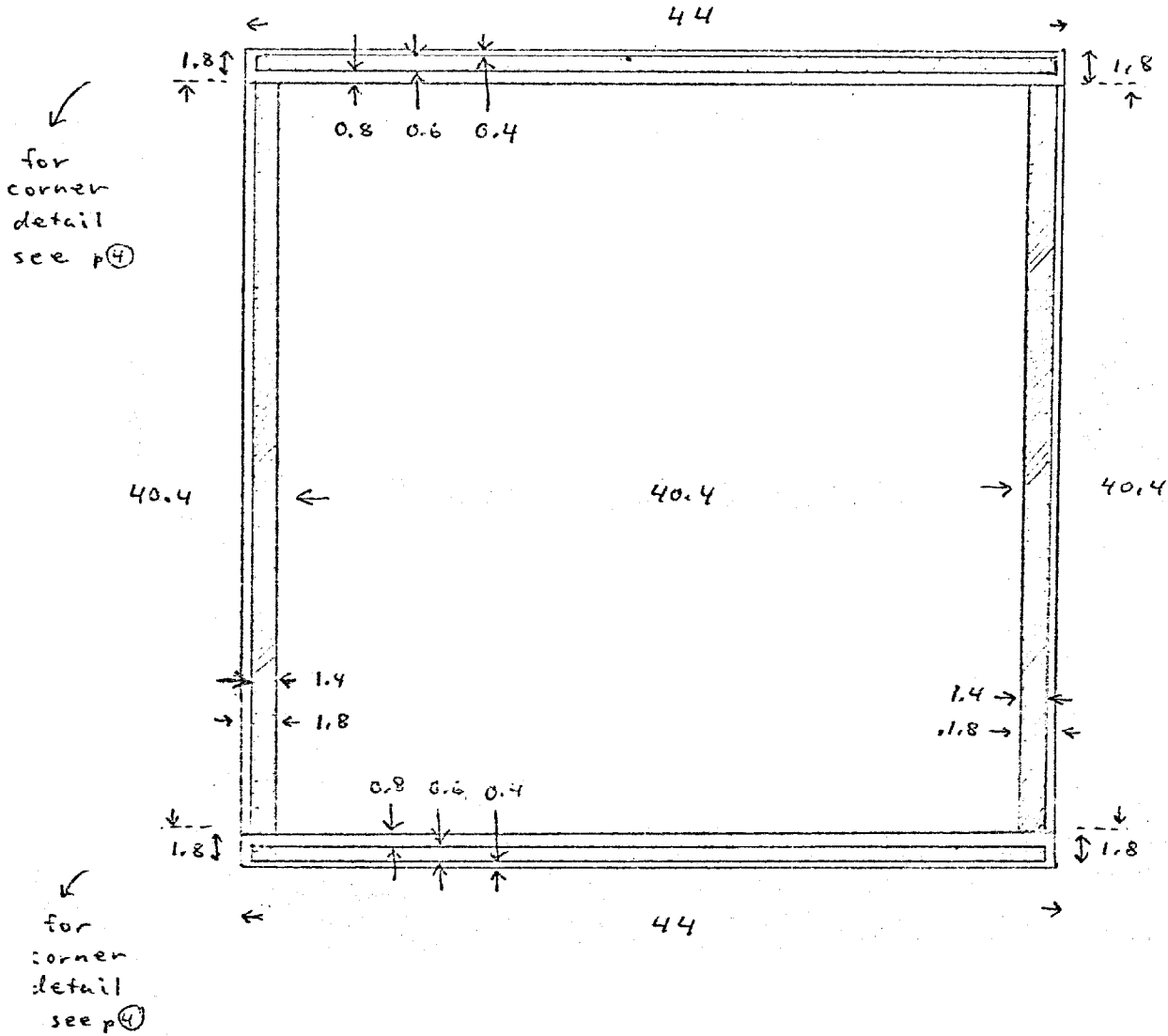Cu - Mylar   4.3

↕ .300

G-10

1.8
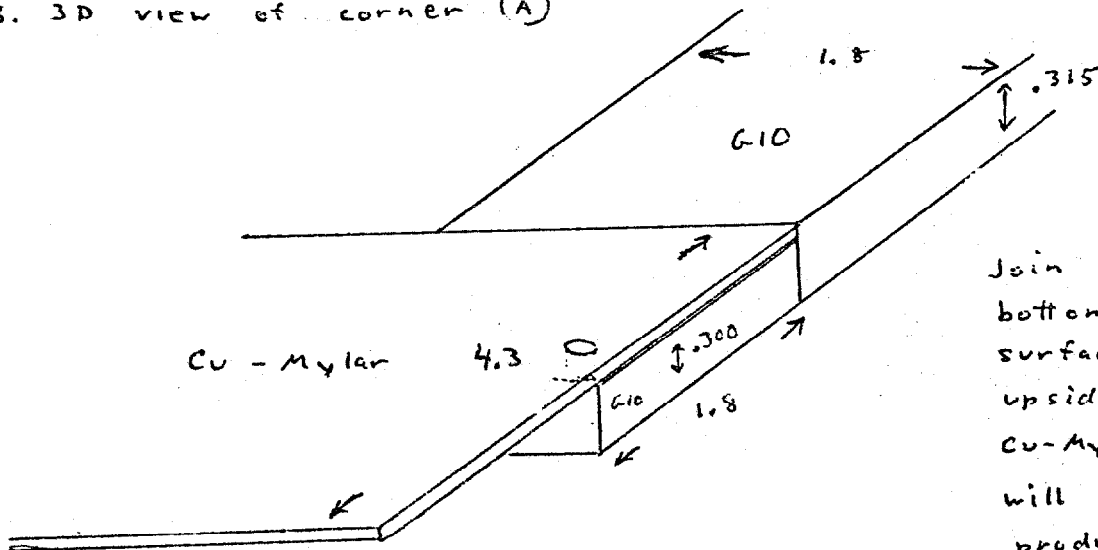
Join G10 pieces with
bottoms flush on
surface plate. Turn
upside down to glue
Cu-Mylar. Epoxy layer
will adjust itself to
produce flush top
surface.

Figure 4

(LBL)

Top G10 Frame

(seen from bottom)

for corner detail see p④

O-ring frame glued to top frame, here shown shaded.

Figure 5

Corner detail, top G-10 frame (seen from bottom)

O-Rings

curve corner

.4 x .270 thick

.6 x (.270 + .005 + .04) thick

.8 x .270 thick   [.045 space for epoxy releif]

wires (attached to bottom frame)

44   ← .4 →   1.4   → ← 40.4 ---   40.4
     (.270   (.270+.005+.04)   (gas volume)
     thick)   thick

(wires shown for orientation only)

.8 x .270 thick   [.045 space for epoxy and solder releif]

.6 x (.270+.005+.04) thick

O-Ring

.4 x .270 thick

44

Figure 6

619 for the 12 in. chamber with 1 plane readout to 219--hopefully--for

the 1 m chamber with 3 plane readout), and we plan to use impulse

soldering for what is left.

2. Uniformity of the outer planes. With only a tensioned fine wire

plane, and that with 5 mm spacing, the stress on the frame was reduced

to the point where the Hexcel was no longer needed for frame support.

(There was less than 0.001 in. sag in 15.7 in.) However when we tried

to do without it, we found the outer planes bulged out too much, under

small to normal gas pressure differences, making the chamber gain highly

non-uniform. Supports of 1/2-in. polyurethane foam sandwiched between

two 15 mil Mylar sheets glued to the Kapton planes made the pulse height

uniform to $\pm$ 10 to 15% over the entire chamber area to within a millimeter

of the edges. When the gap was changed from 2x4 mm to 2x12 mm, signals

2x larger within ~ 1 cm of the edges parallel to the wires and 2x smaller

on the other edges were observed. This was due to the Cu not continuing

over the frame. This edge of the outer plane printed circuit also caused

a small reflection at the point where the delay line crossed it. This

reflection (see Fig. 21) can be removed by placing a Cu strip of the

proper width under the ends of the delay lines in the present chamber,

and by continuing the Cu strips for the full delay line length in the 1m

chambers. We confirmed the observation of Ray Fuzesy[3] that thicker

outside wires and a wire-free space is not needed providing the fine

wires are laid over the frames on each side.

3.   Delay line coupling and the outer planes.

The delay line coupling proved to be much tighter than originally

expected (not that delay lines were different, we just didn't

understand the situation. See section 8 for further details.).   Two

delay lines on the same strips (as occurs for part of the present U

plane) consequently load down the signal.   To prevent this in the

1m chamber the strips are at 45° and only go to one of the two U

plane delay lines.   Along the diagonal, lines of force from

avalanches will still split between strips going to both delay lines.

Figure 7 shows the signal height as a 55_{Fe} source is moved across the
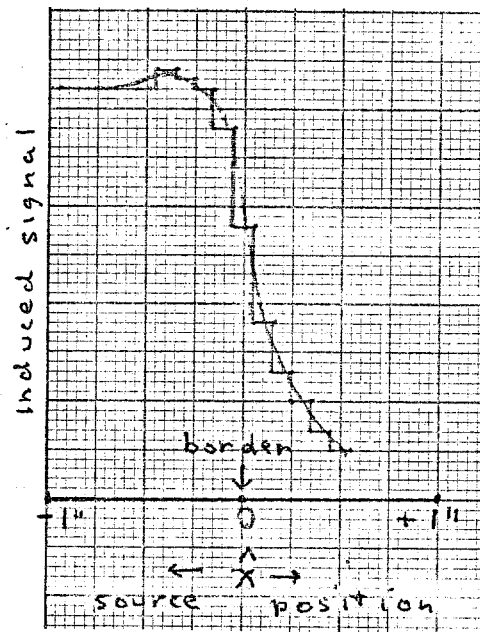
equivalent border in the 20" chamber.

Fig. 7

4.   The central plane

The 20μ central plane has proven to be satisfactory.   The 30μ one

has not yet been tested.   To the extent that the adjacent - wire,

electrostatic instability limits the voltage, a 30μ plane wound

with $(\frac{30}{20})^2$ as much tension would be expected to have a higher

ultimate gain (using the gain formula and data from the uniform -

gain paper[4] together with Tom Trippe's tension formula).   However, that

will not limit us.   The maximum voltage before the instability

sets in is

$$V_{(KV)} \lesssim (980\ T_{(gm)})^{1/2}\ (0.3\ \frac{2\pi(t - s/2) + 2s\ \ln(s/d)}{\left(\frac{V,esu}{KV}\right)\ \ell}) \quad (1)$$

where ℓ = wire length, s = separation, d = diameter, and t = half-gap.[2]

For ℓ = 1026 mm, s = 5 mm, d = 0.02 mm, t = 8 mm, and T = 60 gm, we get

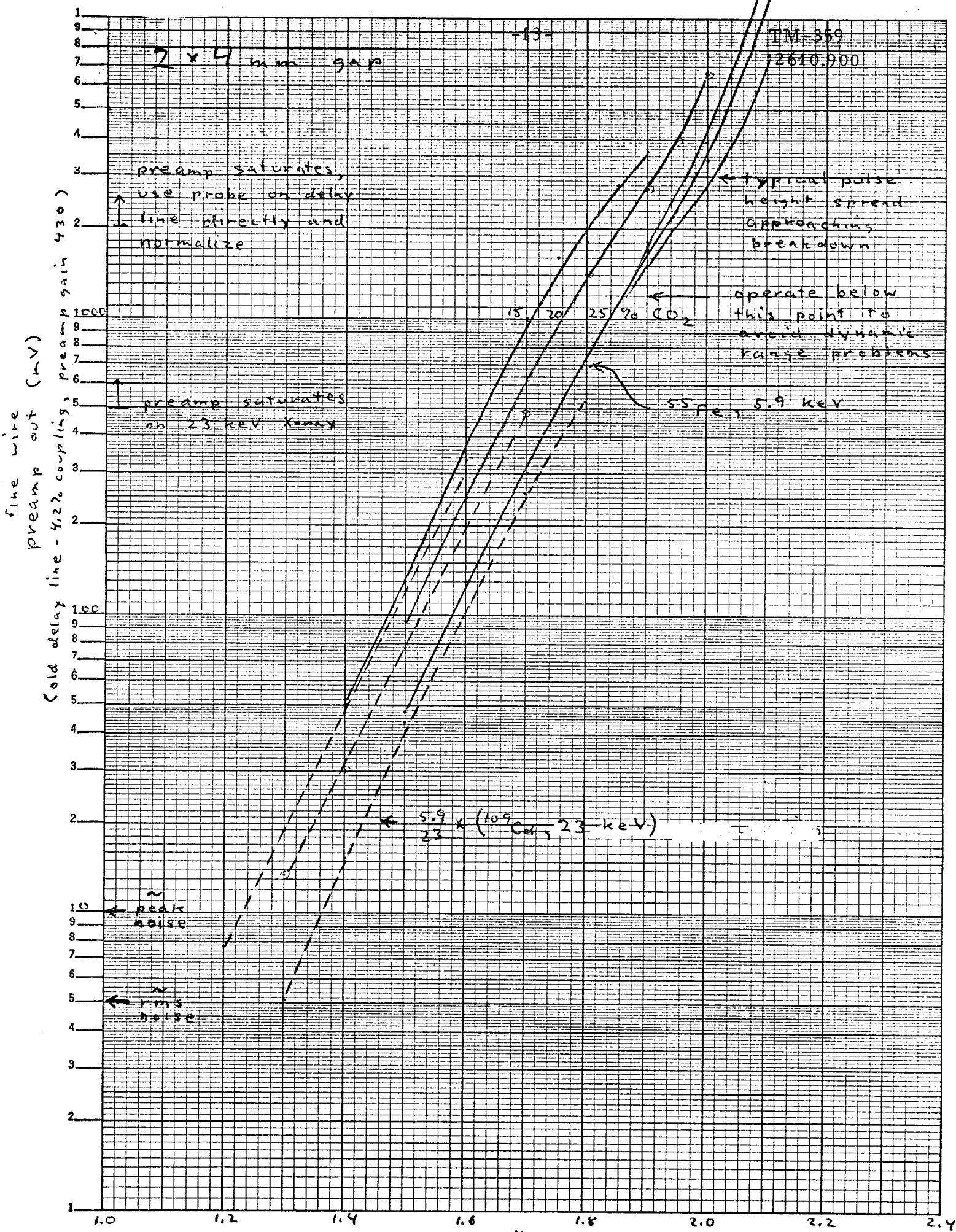$V \leq 6.36$ kV, well above the expected operating range of 2.5 to 3 kV.

5. The Maximum Gain

The gain proved to be limited by regenerative avalanche feedback.

Figure 8 shows [55]Fe signals (85% Ar, 15% CO_2, 2x8 mm gap) as the supply
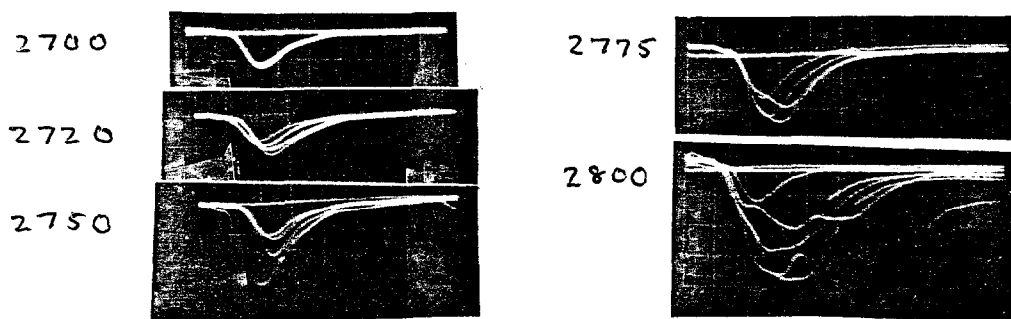
0.2 μs, 5 mV/div; 1:1 probe on end of delay line

Fig. 8

voltage is raised. After more than 600 volts change where the only

obvious effect is an increase in pulse height, a marked increase in pulse

height spread starts at 2720 V. By 2775 there is an increase in pulse

duration as well. If the voltage is increased beyond 2800 V, the

regenerative processes (ionization by ultra-violet photons and possibly

ions that have traveled away from the wire) cause continuous discharges.

The increased pulse height spread is presumably also caused by an earlier

stage of the same phenomena. Figures 9 to 13 show the gain for 2x4, 8,

and 12 mm gaps; 15, 20, 25, and 30 % CO_2; and [55]Fe (5.9 keV x-rays),

[109]Cd (23 keV x-rays), and [90]Sr (2.26 MeV collimated β's passing through

Fig. 9 — Signal vs HV

Axis labels:
- Y-axis: fine wire preamp out (mV) (old delay line – 472% coupling, preamp gain 430)
- X-axis: HV (kV)

Handwritten annotations on figure:
- 2 × 4 mm gap
- preamp saturates, use probe on delay line directly and normalize
- preamp saturates on 23 keV X-ray
- ~ peak noise
- ~ rms noise
- $\frac{5.9}{23} \times (^{109}Cd, 23\,keV)$
- 18 20 25 % CO_2
- ← typical pulse height spread approaching breakdown
- operate below this point to avoid dynamic range problems
- ^{55}Fe, 5.9 keV

2 x 8 mm gap

typical pulse height spreading approaching breakdown

$\leftarrow$ ^{55}Fe, 5.9 keV

15   20   25   30 $\%$ CO_2

$\leftarrow \frac{5.9}{23} * (log_{10}, 23 \text{ keV})$

preamp out (mV)

Fig. 10 - Signal vs HV

kV

Fig. 11 - Signal vs HV

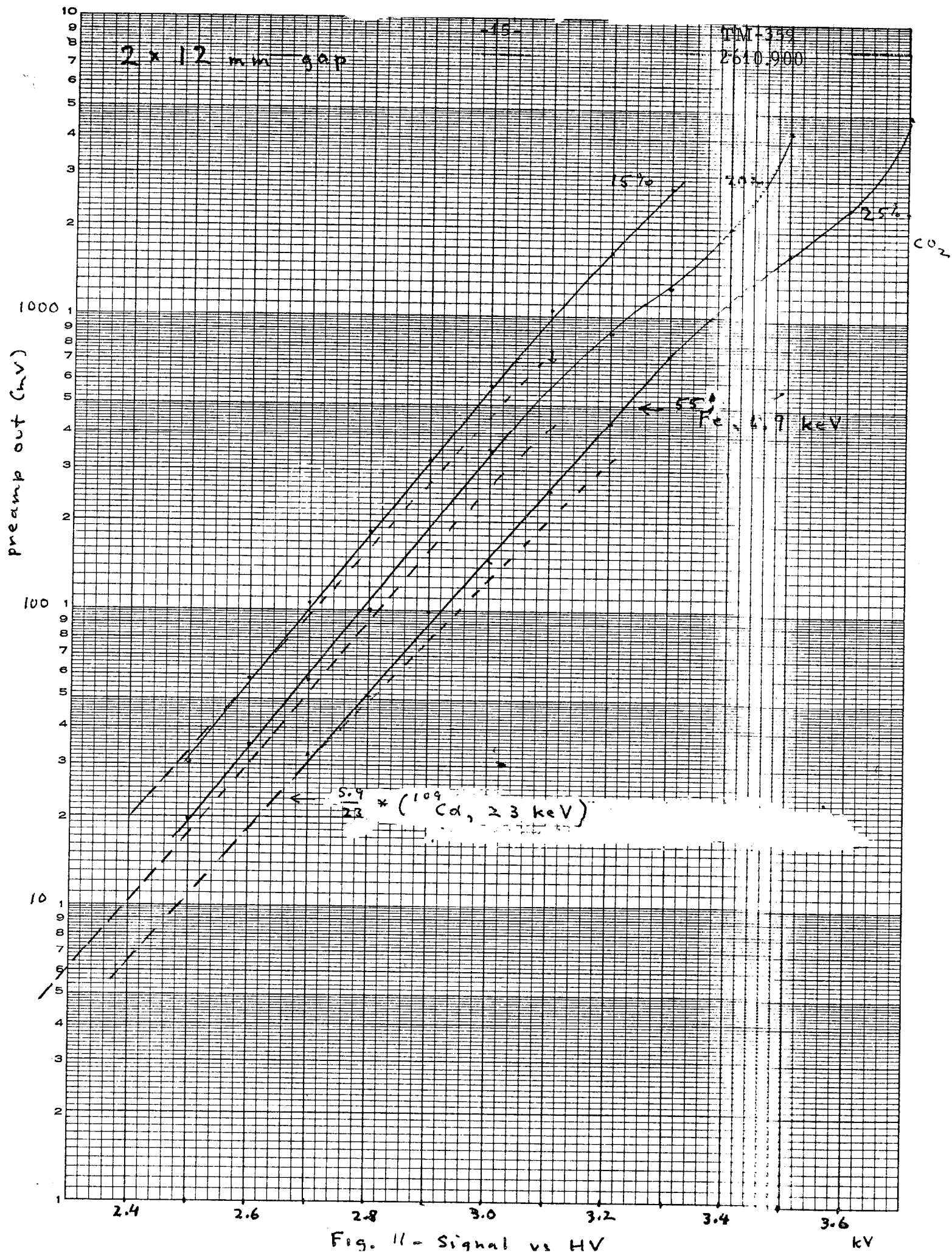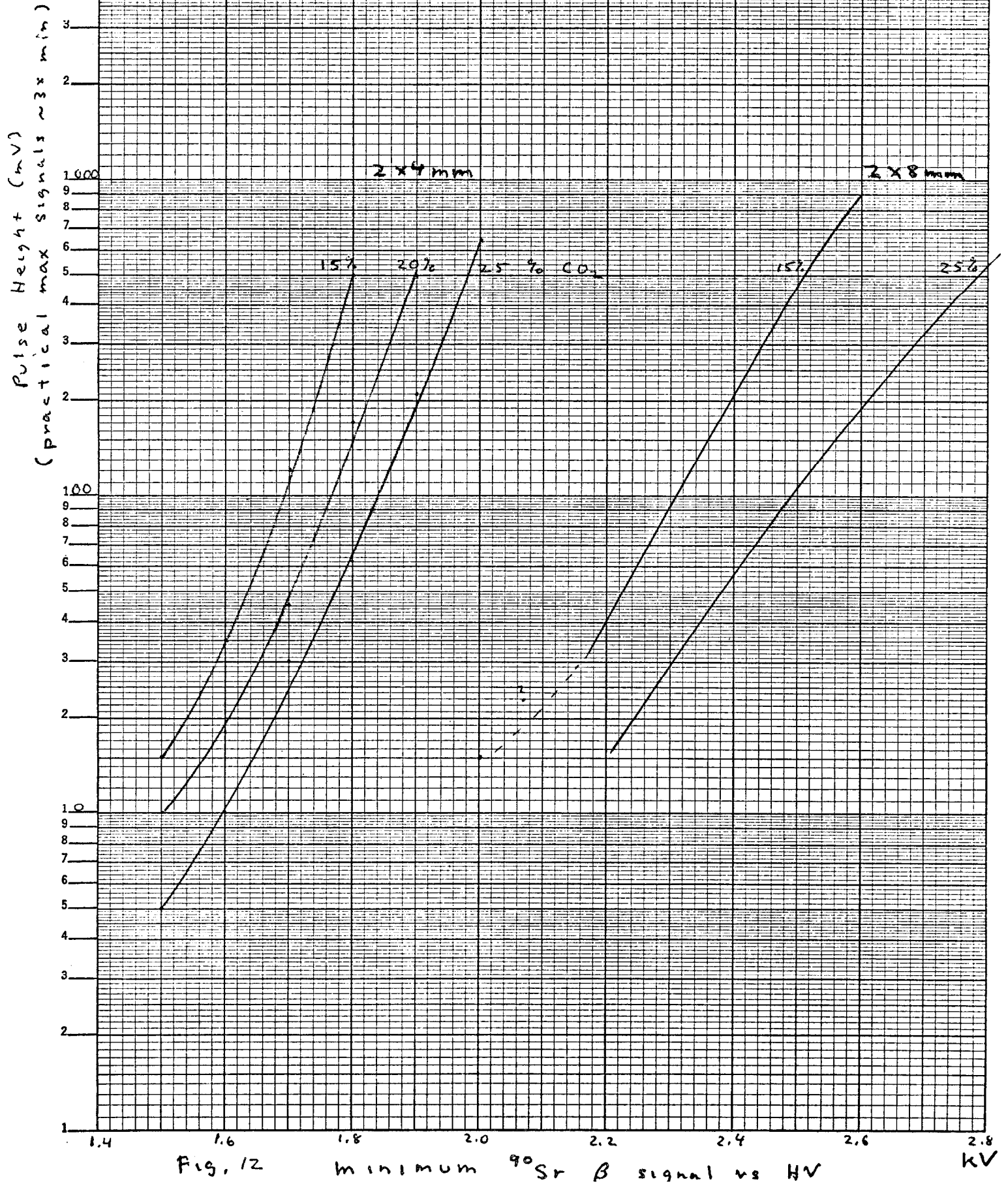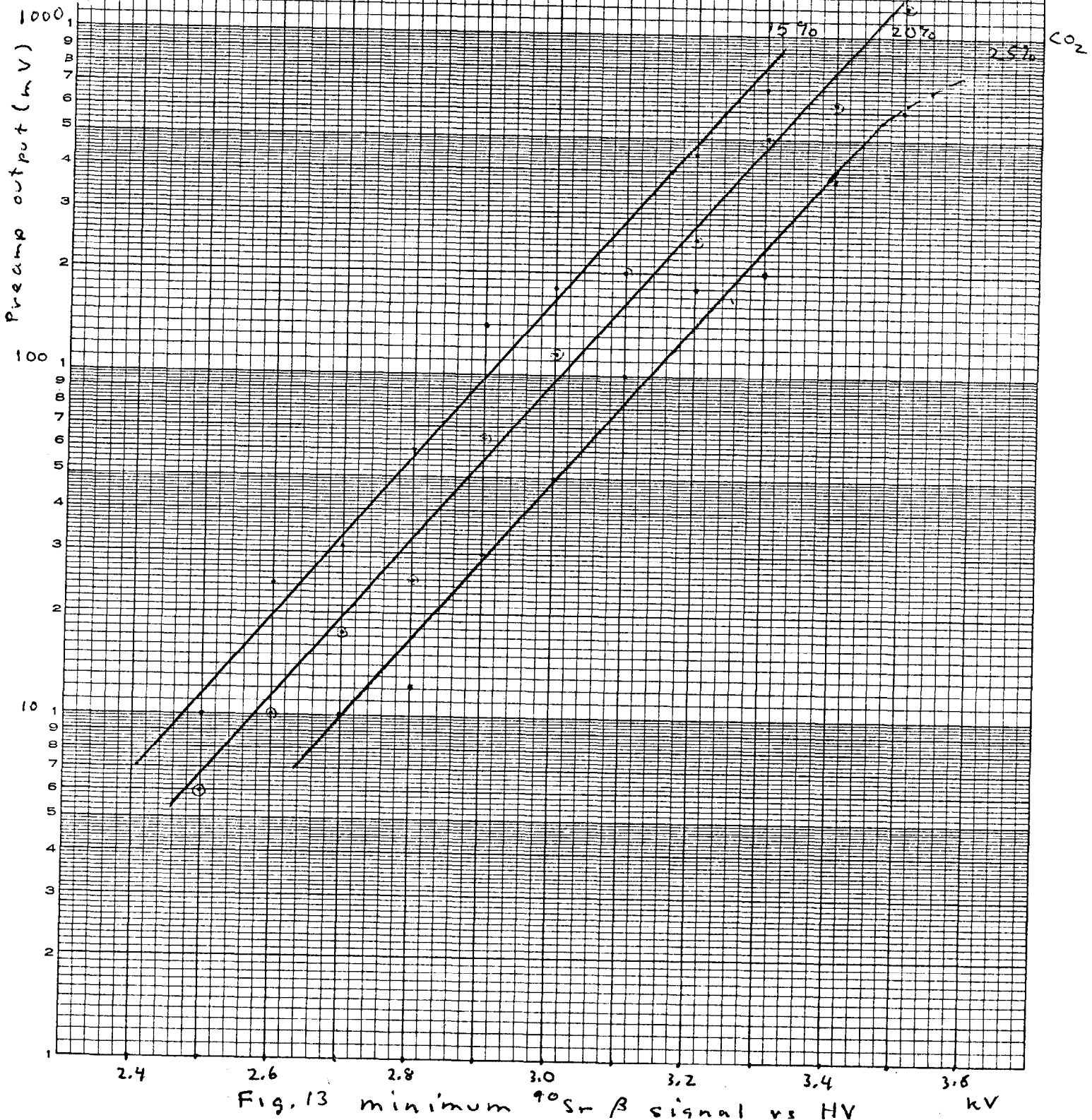Fig. 12   minimum ^{90}Sr β signal vs HV

Fig. 13 minimum ^{90}Sr β signal vs HV

the chamber and triggering a scintillator below it). Since we need

100% efficiency, the minimum β pulse height is plotted; pulses of up to

three times that are common because of Landau straggling. Despite the

factor of two in maximum high voltage as the gap is varied from 2x4 to

2x12 mm the maximum attainable pulse height is the same within measure-

ment errors. In all cases the approach to breakdown is qualitatively

unchanged from Fig. 8.

When the percentage of CO_2 is increased, the gain drops, presumably

from an increase in inelastic, non-ionizing collisions. An ~ 8% increase

in voltage is necessary to restore the gain when the CO_2 is increased

from 15% to 25%. Now, however, it is possible to raise the voltage still

further and get a larger ultimate gain since an increased fraction of the

photons that could start new avalanches are being absorbed in exciting

(but not ionizing) CO_2.

Several other features of the curves are of some interest. A

comparison of the 23 keV and 5.9 keV x-rays shows proportionality of gain

at low values and the onset of space charge saturation at the higher

values. This probably also causes the reduction from the exponential

voltage dependence of the ^{55}Fe pulse height since the simple theory that

predicts a near straight line (see formula and references in uniform gain

paper)[4] allows for neither space charge nor regenerative effects.

The source-off counting rate is voltage independent to within 200

volts of breakdown providing the counting threshold is set at a constant

fraction of the ^{55}Fe pulse height. For 10, 50, and 100% of 5.9 keV, it

was measured to be 76, 54, and 43 counts/second. These numbers include

counts from approximately 27 cosmic rays/second and do depend somewhat

on the state of cleanliness of the chamber. Guard strips have never

been tried, are presumably unnecessary, and would complicate the constr-

uction. Wires finer than 20μ would probably allow a yet higher maximum

gain, so long as the electrostatic-force limit is not exceeded. At one

extreme, it is known that a parallel plate, DC proportional chamber

cannot be made; it breaks down. On the other, Rich Muller and Steve

Derenzo, using 3.6 and 5μ dia. wire have reached gas gains in pure xenon

--no quencher at all--of over $40,000.^5$ The best we have done in pure

argon with 20μ wires is 100. Finally, we had all sorts of trouble with

breakdown in the field intensification region of the gas tubes in our

lead-plate spark chambers when we had large diameter holes. Smaller

holes with their necessarily greater intensification, nevertheless, gave

no trouble. All this leads one to suspect that minimizing the volume of

gas in high fields may be desirable. Someday, after we have experience

in winding and operating 20% chambers, it might be desirable to try one

with 10 to 15μ wire. No other accompanying changes would be needed,

providing the tensioning device could handle this range.

6. Selection of the Gap Thickness

The maximum measured gas gain does not change significantly with

gap. However, the track length is proportional to the gap, and since we

do not use electro-negative gasses, we collect all the electrons. Also,

since the delay lines sum and interpolate to find the center of inclined

tracks, the usual multiple signal problem with individual wire readout

is not present. Larger gaps, in addition, reduce the sensitivity of the

gain to gap non-uniformities. Examination of Figs. 9 to 13 indicates

that for a constant output voltage, V_{supply}/t decreases as the half

gap, t, is increased. From formula (1) it can be seen that such a

decrease makes the tension requirement less stringent.

What finally sets an upper limit to the gaps is a completely

different phenomena: incoherent addition of the induced pulse at the

delay line. The field induced by the positive ions pulling away from the

central wires is spread over a length comparable to the gap thickness

when it reaches the outer plane. Figure 14 shows the measured spread for
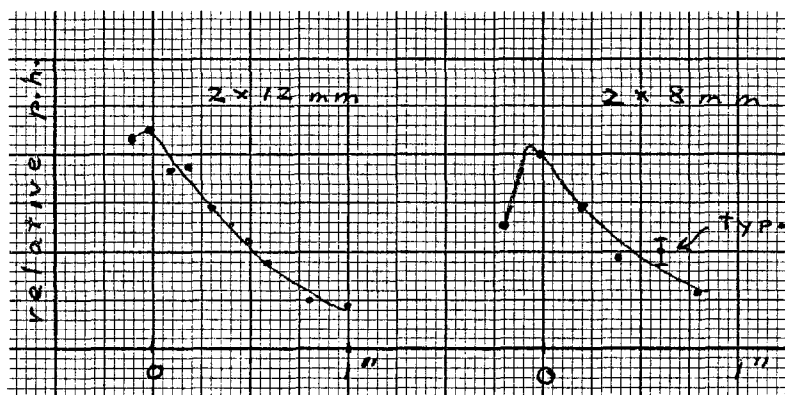
2×8 and 2×12 mm gaps.

Figure 14

When this distance becomes comparable to $(v_{delay\ line}) \times (\tau_{pulse\ width})$

the induced signal amplitude decreases. For 2×4, 8, and 12 mm gaps the

induced signal was 33, 40, and 15% of the wire plane signal. (Our 12 in.

chamber gave 40 $^o/o$.) The maximum expected is ~ 50 $^o/o$ / $0.65 \approx 75$ $^o/o$.

(50 $^o/o$ because half of the lines of force go to the other cathode plane,

and 0.65 because the central fine wire signal is reduced by that factor due

to the addition at the delay line of induced pulses of the opposite sign

from adjacent wires.) The ratio for 2x8 mm is quite satisfactory, however,

the 2x12 mm ratio, combined with the other major sources of

pulse height spread, the Landau effect (3:1), delay line attenuation

(at least 2:1) and track length variations (say 1.5:1) would present

the amplifiers with a required dynamic range of 60:1; possible, but very

uncomfortable. One question remains: why is the ratio down to 33% at

gap, t, is increased. From formula (1) it can be seen that such a

decrease makes the tension requirement less stringent.

What finally sets an upper limit to the gaps is a completely

different phenomena; incoherent addition of the induced pulse at the

delay line. The field induced by the positive ions pulling away from the

central wires is spread over a length comparable to the gap thickness

when it reaches the outer plane. Figure 14 shows the measured spread for
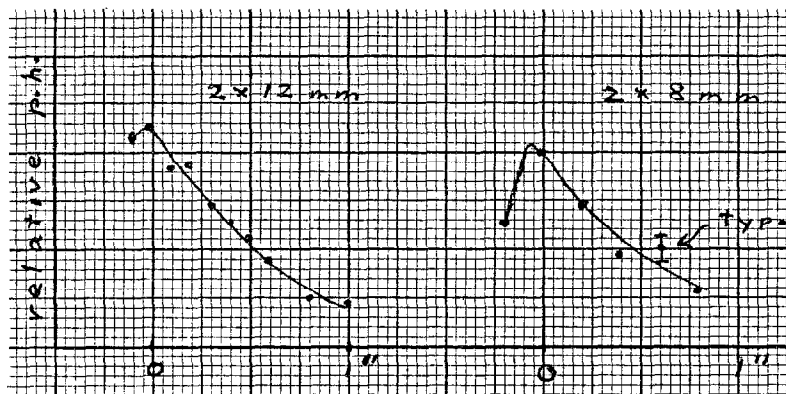
2×8 and 2×12 mm gaps.

Figure 14

When this distance becomes comparable to $(v_{delay\ line}) \times (\tau_{pulse\ width})$

the induced signal amplitude decreases. For 2×4, 8, and 12 mm gaps the

induced signal was 33, 40, and 15% of the wire plane signal. (Our 12 in.

chamber gave 40 $^{o}/o$.) The maximum expected is $\sim 50\ ^{o}/o\ /\ 0.65 \approx 75\ ^{o}/o$.

(50 $^{o}/o$ because half of the lines of force go to the other cathode plane,

and 0.65 because the central fine wire signal is reduced by that factor due

to the addition at the delay line of induced pulses of the opposite sign

from adjacent wires.) The ratio for 2x8 mm is quite satisfactory, however,

the 2x12 mm ratio, combined with the other major sources of

pulse height spread, the Landau effect (3:1), delay line attenuation

(at least 2:1) and track length variations (say 1.5:1) would present

the amplifiers with a required dynamic range of 60:1; possible, but very

uncomfortable. One question remains: why is the ratio down to 33% at

2 x 4 mm. It's not clear. It may be part measurement error, part reduced

coupling at the delay line, since the signal comes in on fewer strips and

hence sees a lower capacity to the delay line.

7. Efficiency

The efficiency for all gaps was measured to be 100% with an error of

1/2%, and thus played no role in chamber design. The scope was triggered

on ^{90}Sr counts from a scintillator under the chamber. Half-inch lead

collimators were used both above and below the chamber. A definite

minimum β pulse height was seen (see Fig. 15.) Occasional zero height

pulses were also seen at a rate compatible with the phototube noise rate.

Two typical runs of equal duration at 2 × 8 mm gave:

1115 triggers, collimator open - 1102 counts + 13 zero height traces

54 triggers, collimator closed - 38 counts + 16 zero height traces
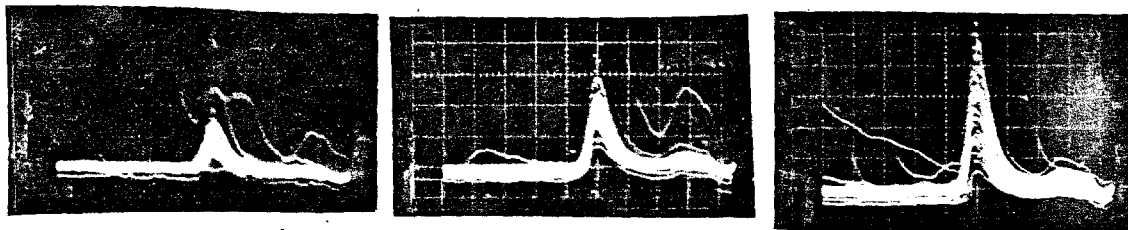
50 traces each -->   2.6 kV, .2V/div   2.8 kV, .5V/div
2.4 kV, .1V
                              Figure 15

β pulses (triggered by scint.), 2 × 8 mm gap, 25% CO_2, x = 5.6 in.

y = 11.4 in., .5μs/div

8. Delay line performance

The use of flexible circuit boards clamped to the delay lines has

produced a reliable coupling. The delay line that is placed on the high

voltage plane is wrapped with three turns of 1/2 mil Mylar and kept at

ground. (It is much easier to make the transition from high voltage in

the high impedance part of the circuit. When the signal is on the

~ 1 kΩ delay line, headed for a

~ 1kΩ termination, any series capacitor must have $1/\omega C \ll 1K\Omega$. Disc

ceramics are rather noisy and glass encased ones in that capacity and voltage

range are large, expensive, and a general nuisance.)

Figure 16a shows ^{55}Fe pulses from one end of the wire plane delay

line when the scope is triggered by the other end. Due to the quanti-

zation of the avalanche positions by the wires, the pulses come out at

discrete positions with the only scatter being at ± 0.2 mm spread due

to noise.
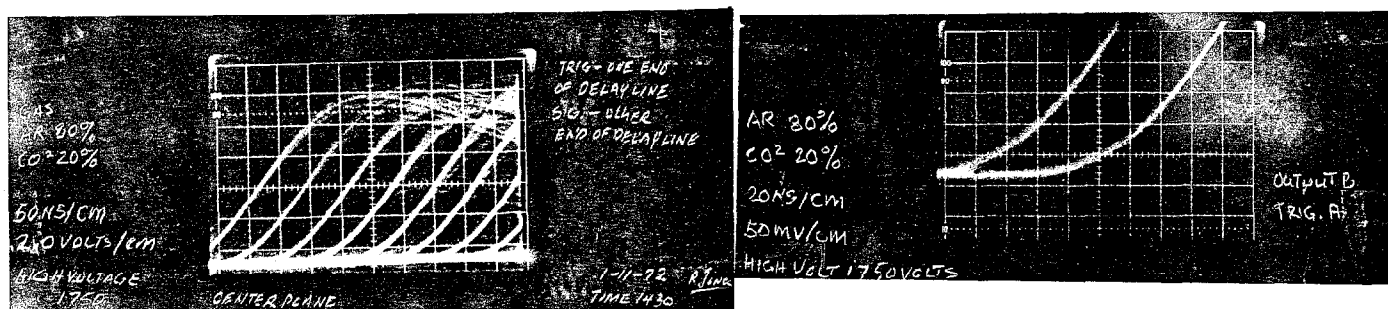
2 × 4 mm gap, 20% CO_2, 1.75 kV,   20 nsc/div
50 ns/div

Figure 16a

Figure 16b shows similar pulses from the induced plane (Y) delay line

for two positions of the source separated by 1 cm. Now a spread about

each position of about ± 1.5 mm can be seen. This is reasonable consider-

ing the dimensions of the source.

Fig. 16b. 2 × 4 mm gap, 20% CO_2, 1.7 kV, 0.1V/div, 50 ns/div, ^{55}Fe

The delay line* coupling was measured by taking the ratio

*Original 20 in. delay lines (1/4 by 3/4 by 20 in., 3/4 in. wide ground,
No. 36 wire, 7.0 ns/mm).

$$\frac{V, \ 1\!:\!1 \text{ scope probe at delay line end}}{V, \ 1\!:\!1 \text{ probe on printed circuit pad}} = \frac{1.8 \text{ mV}}{11.5 \text{ mV}}$$

The delay line and preamplifier were in place for both measurements. This figure includes the normal (small) attenuation for the last few inches of the delay line, but does not include a correction for the extra loading of the pad signal by the probe capacity. This is measured by measuring

$$\frac{V, \text{ preamp, probe on pad}}{V, \text{ preamp, probe off}} = \frac{145 \text{ mV}}{434 \text{ mV}}$$

The final result is then $(1.8 \times 145)/(11.5 \times 434) = 5.3\%$.[*] A similar measurement with the same delay line wrapped with Mylar for high voltage service gave 4.2%. Attempts that have been made to increase this figure by doing such things as scraping off the insulation and soldering the delay line wires to the pads would not be expected to have much effect however, (other than wrecking the delay line) because the capacitative coupling to the delay line is already quite tight. This showed up clearly when we tried to take a prompt signal out by looking at the end of the $470 \text{ k}\Omega$ resistors as shown in Fig. 17.
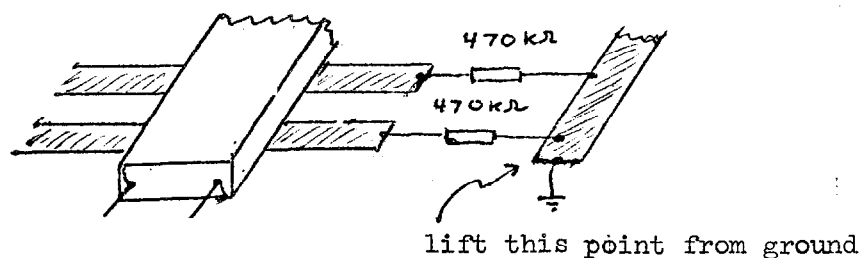

lift this point from ground

Figure 17

[*]The coupling for the new delay lines (3/16 by 1 by 20-in., 0.5 in. wide ground, No. 38 wire, 7 ns/mm) is greater by a factor of 10/9.

Nothing came out! Not until the 470kΩ was reduced to the point

where the delay line signal was being degraded (due to the low, position

dependent, shunt impedance of all the parallel resistors), was much

signal seen. Clearly most of the current was going into the delay line.

This was also seen on the U plane. Those strips that ran to 2 delay

lines produced a signal only 1/3 as large (see Fig. 18).
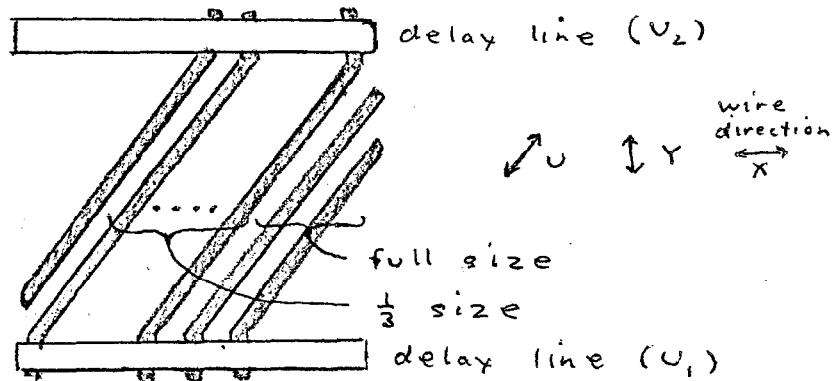

Figure 18

This would not happen if the delay line were only loosely coupled

to the pad. The coupling capacitance can be measured by driving a

single pad with a pulse that is long compared to the delay line length,

attaching a 10:1 probe to the delay line and observing the RC decay

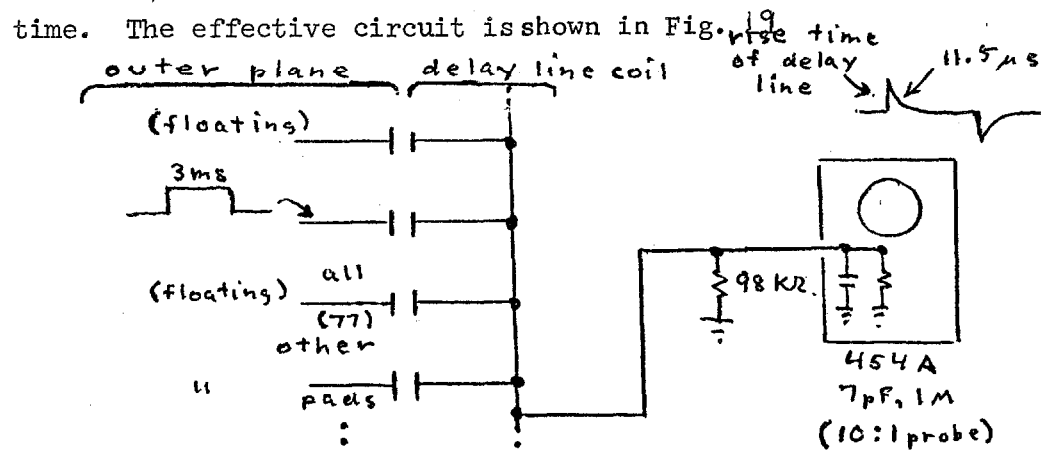time. The effective circuit is shown in Fig. 19.

Figure 19

The pulse rises with the delay line rise time (100 ns) since the pulser

driving impedance times 7pF is relatively short. It falls with a time

constant 98 KΩ $\times$ $C_{(pad - delay line)}$ = 11.5 μs giving $C_{(pad-delayline)}$

equal to 117 pF. This is not unreasonable; an air filled, parallel

plate capacitor of the same area and capacity would have a gap of 0.15

mils which is comparable to the wire insulation thickness. The pads on

the fine wire plane are twice as wide, so the coupling there should be

$\sim$ 234 pF. The impedance of this coupling is

$$|z| = 1/\omega C \simeq \frac{1}{(1.6 \times 10^{7})(234 \times 10^{-12})} = 270 \, \Omega$$

which is low compared to every other impedance around. Since the induced

plane signal comes in on about 20 strips (see Fig. 14), its coupling

impedance is even lower. The reason for the coupling efficiency as

defined earlier $(V_{delay\ line}/V_{chamber})$ being less than 1 is that the

chamber is a current source. A certain number of positive ions are

moving away from the wires at a rate determined by the high voltage.

Electrons are being released from the anode wires, pass through the

power supply and go to the cathode plane where they are attracted by the

approaching positive ions. The delay line is in series with this circuit

(for fast AC signals), so the signal voltage will be $\sim$ I(z/λ) where z,

the delay line impedance is only $\sim$ 1kΩ(currently).

Several sources of spurious pulses have been found and removed. On

the Y = max side of the chamber, the Y and U_2 delay lines are adjacent,

and signals jumped between them until we placed two sheets of bakelite

surrounding one of copper between them. An interesting effect was seen

when the U plane was not tied down with a delay line: a displaced pulse

on the Y plane delay line whose position, relative to the main pulse,

depended on the position of the source along the strip being read out

(see Fig. 2).

express paths:
source → U strip →
Y strips → delay
line ahead of
normal entrance
point

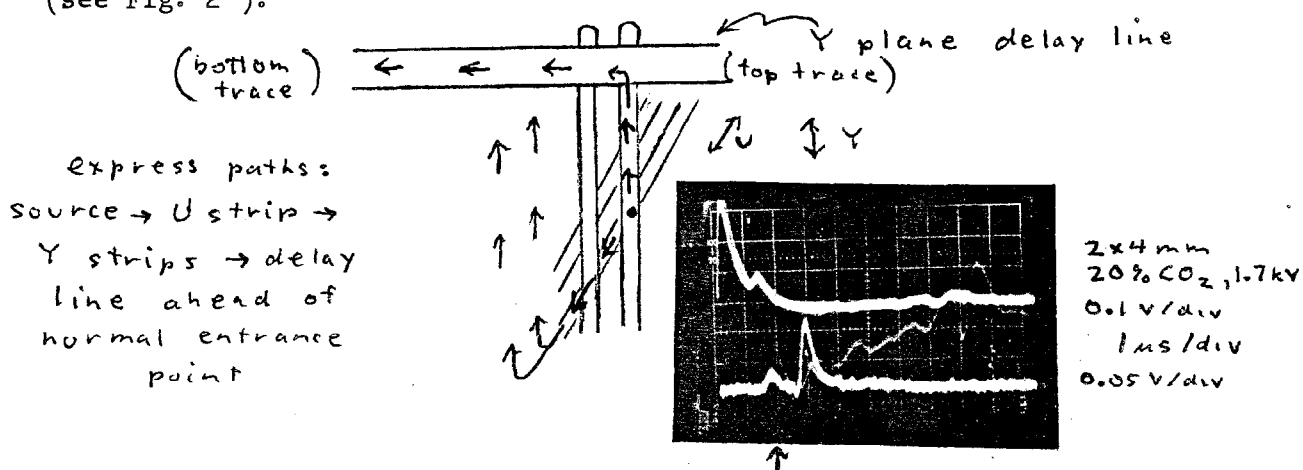2x4 mm
20% CO_2, 1.7kV
0.1 v/div
1 μs/div
0.05 v/div

Figure 20

The jump from the U plane to the Y plane is made capacitatively.

Figure 21 shows a reflection caused by the edge of the copper

plating and by the end of the delay line 2 in. further on.   A, B, and C

show the end reflection change as the terminating resistance is varied.

x term small   x term OK   x term large

A   B   C

2x4 mm gap, 20% CO_2, 1.7 kV, wire plane (x) delay line ($\frac{3}{4}$" line)
top trace y = min end (trig. scope).
bottom trace y = max end   0.2 V/div, 1 μs/div

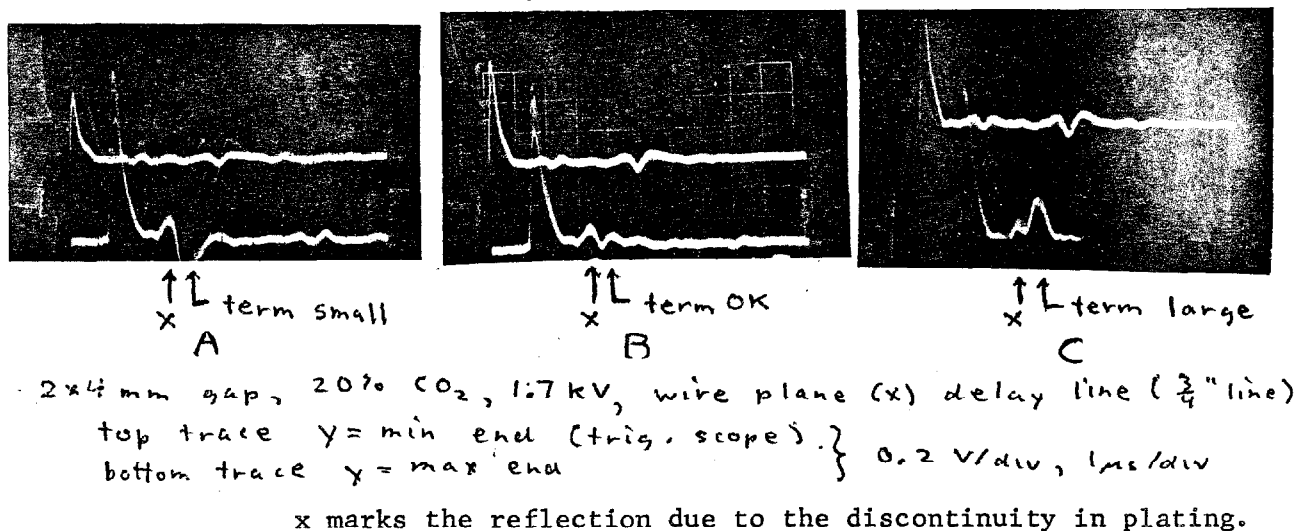x marks the reflection due to the discontinuity in plating.

Figure 21

The reflection at x is removed by inserting a grounded Cu strip halfway

under the delay line. (When it is pushed under further, the reflection

reappears.)

9. Prompt signal

Up to now we have gotten prompt signals from scientillators or from an unused plane (cathode or anode) from the proportional chamber. Neither will be possible with the EMI, and getting a good prompt output without interfering the other three (X,Y,U) has proven to be non-trivial. Looking at the cathode common bus (Fig. 17) did not work well for reasons mentioned in section 8. A 1" wide Cu strip laid over the pads and separated from them by 2 mils of Mylar gave a good signal but degraded the rise time and peak amplitude of the delay line signal. The most promising method picks off a signal from the delay line ground.

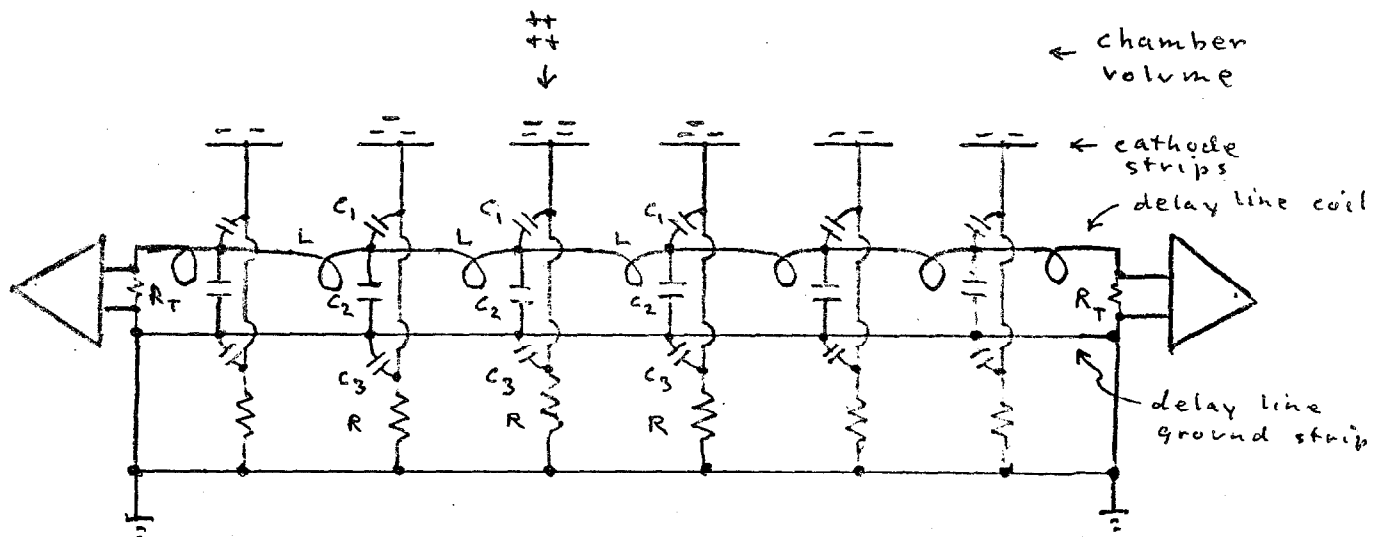Consider the equivalent delay line shown in Figure 22.
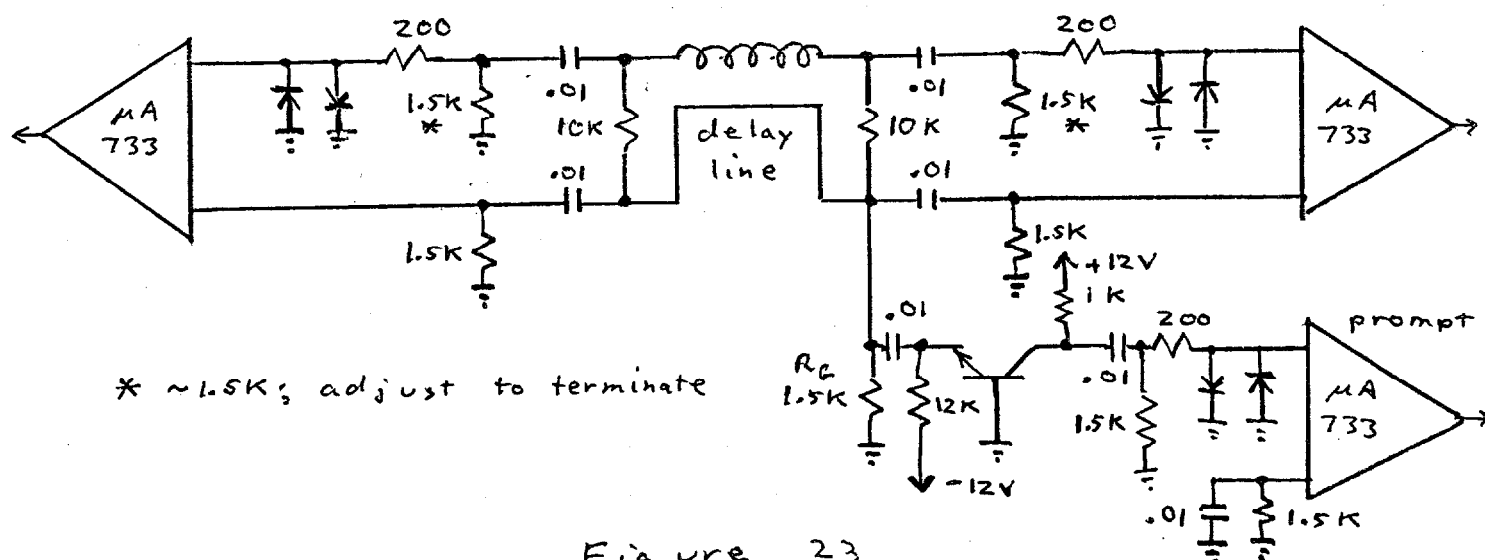

Figure 22

When positive ions in the chamber approach the cathode strips, both the ground and the coil of that part of the delay line tend to experience an increase in potential since they are coupled to it through the initially uncharged capacities C_1 and C_3. Due to the ground strip's low resistance and inductance, electrons travel rapidly along it toward the positive ions, keeping it at ground.

The potential of the cathode strips near the ions and of the coil near

those cathode strips swings positive as the ground current passes through

and charges the capacities C_2 and C_3. A signal then propagates slowly

along the delay line as the C_2's discharge through the L's. C_1 is large,

and so the coil and cathode strips tend to follow each other. Eventually,

the charge on the cathode leaks off through the large resistors R.

Now suppose the delay line ground strip is lifted from ground, as

shown in Fig. 23, by resistor R_G. The ground strip current can now

generate a prompt voltage signal. Both imputs to each delayed signal

amplifier rise as the distributed capacitances are charged. (The inputs

are tied together initially mainly by the C_2's (fig. 22).) Since the

amplifier is a differential one, and has, in its output stage, a filter

to block high frequencies, the prompt signal is suppressed. To complete

the suppression it is necessary to add a common base input to the prompt

amplifier to reduce its input impedance ($z_{in} \sim 50\Omega$) and hence the voltage

swing of the delay line ground strip. The 0.01 µF low voltage capacitors

shown prevent the DC bias currents of one amplifier from affecting the

others. The diodes protect the Fairchild µA733 IC's from large voltage

swings. The 10K's provide a DC return.

Full details of the delay line amplifiers are shown in Fig. 24.

They were designed by Kai Lee, who also suggested using the ground strip

pickoff.

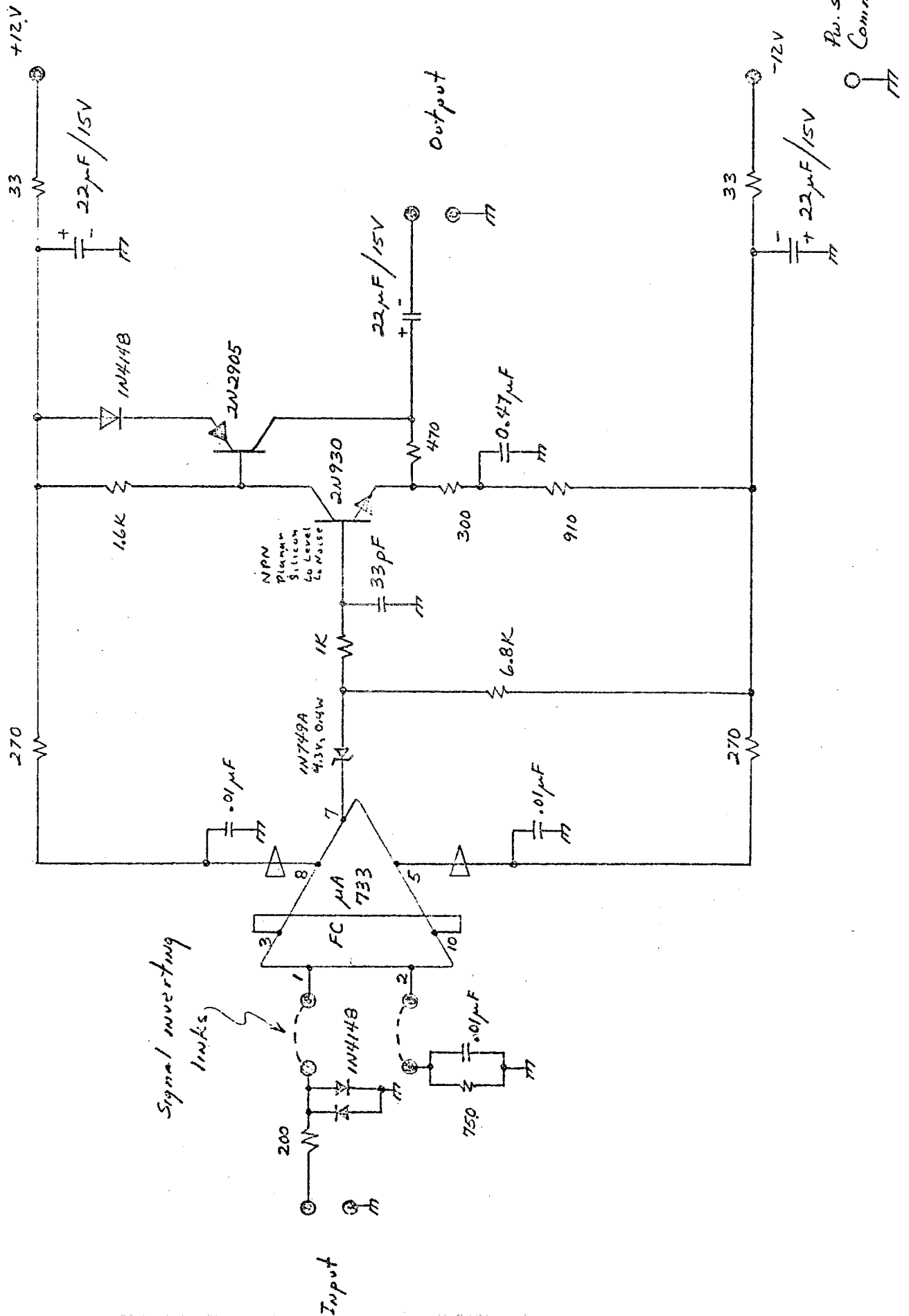* ~1.5K; adjust to terminate

Figure 23

Figure 24

MWPC Pre-amp. (x100)

Figure 25a shows the prompt and delayed outputs from the wire plane delay line. Attenuation along the delay line (new type) can be seen, comparing the y = 12 in., 9 in., 6 in., and 3 in. traces.
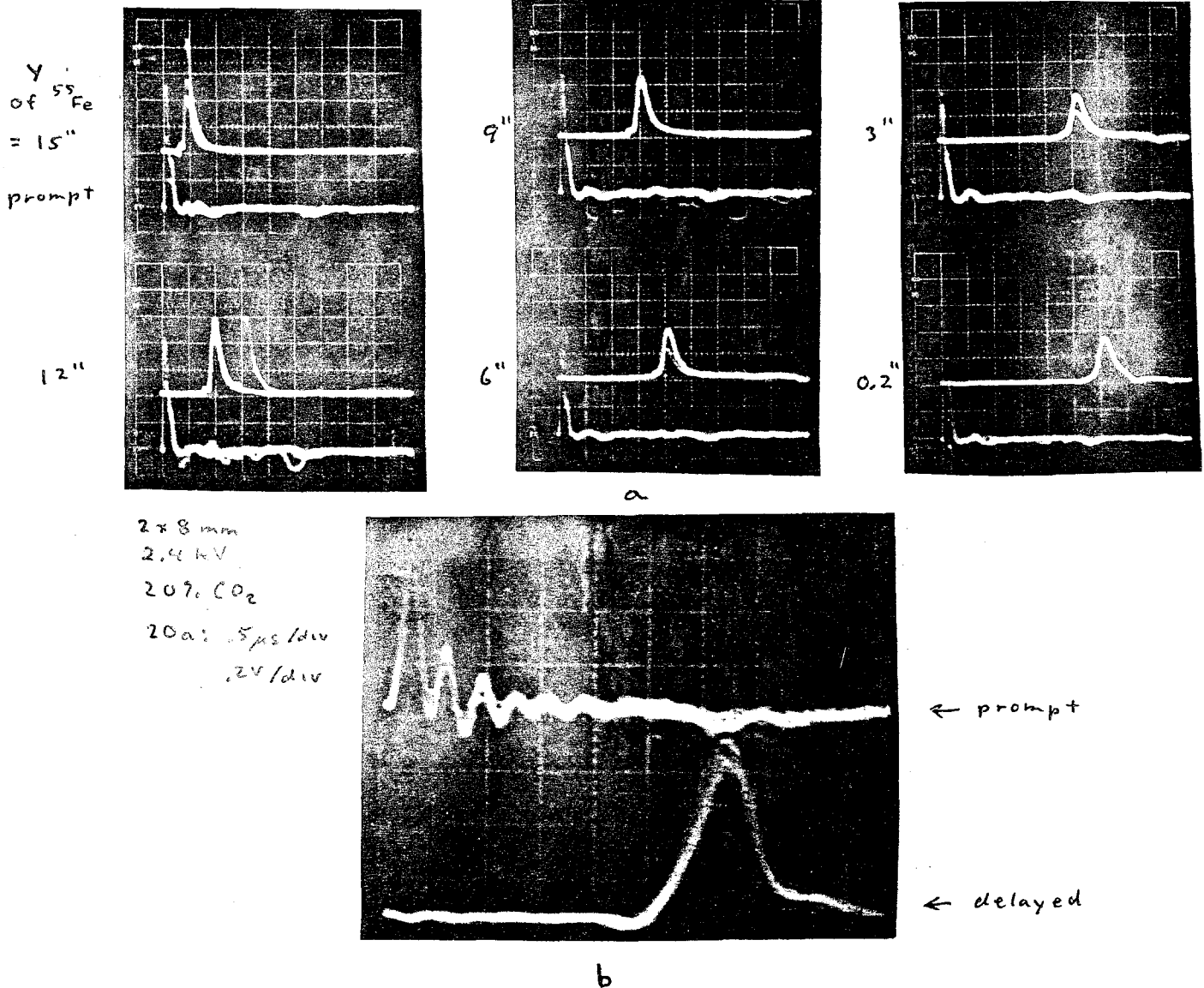

Figure 25

Initially the small ringing on the prompt output was far worse (see Fig. 25b). This turned out to be due to one of the two U plane delay lines being off at the time the tests were started. The source was nowhere near the affected section, but the signal took two capacitative jumps following paths such as the one shown in Fig. 26. As the delayed signal progressed down the structure composed of the delay line,

capacitances C_1, and the Y plane strips, similar paths were created, causing the observed ringing.

Figure 27 shows the signals before and after 400' of RG 55U coax. The cost for this cable is 6¢ per foot. RG 58U which is similar (17.8 db/100 ft. at 10^9 Hz vs 16 db for RG 55U) costs 3.2¢ per foot.
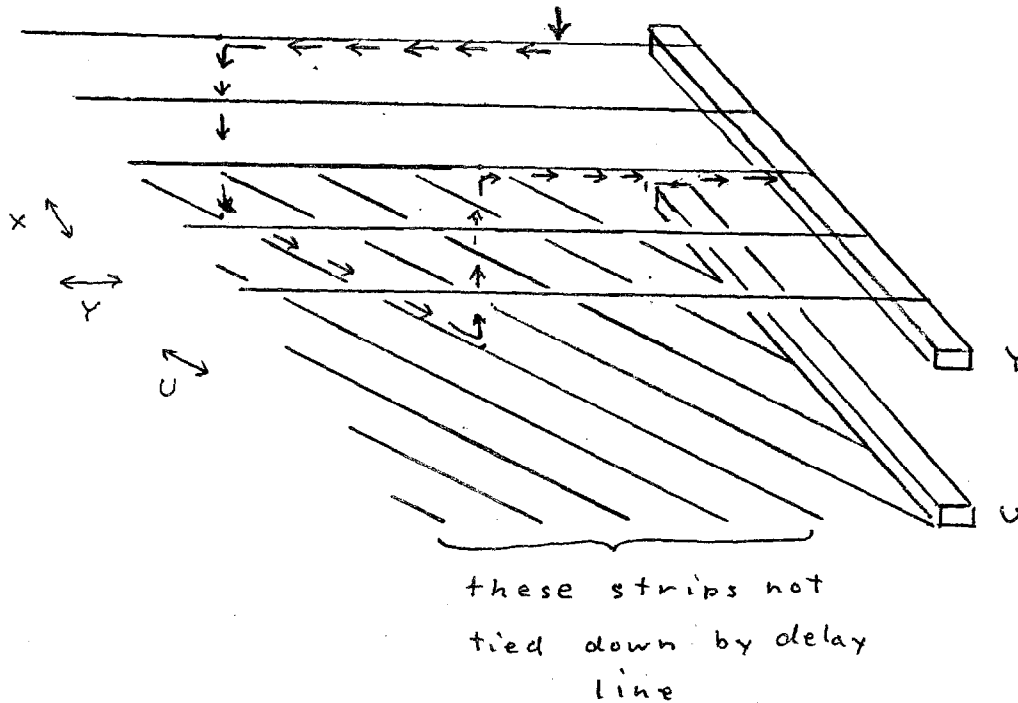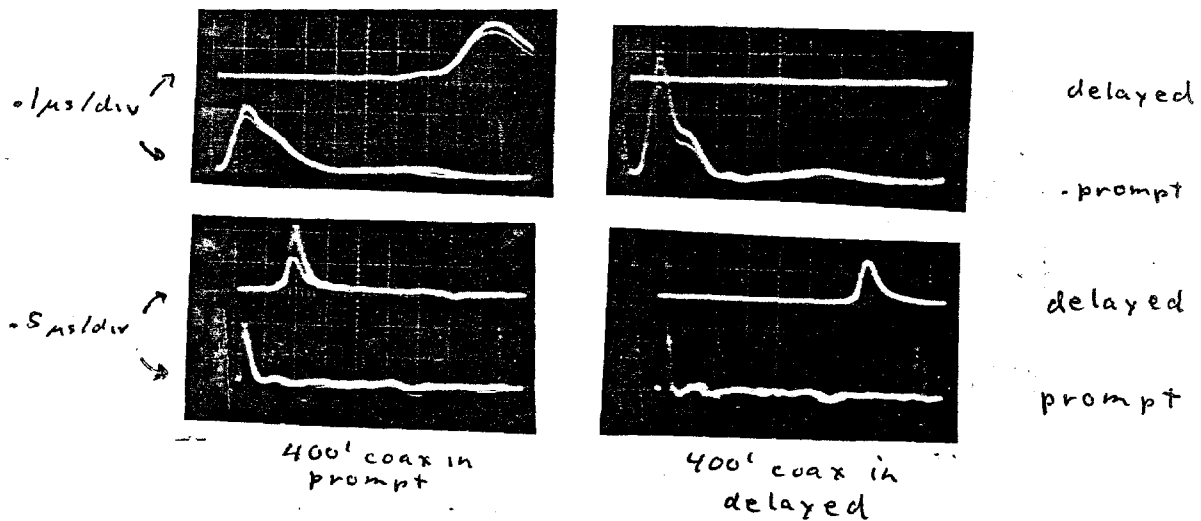

these strips not tied down by delay line

Figure 26

delayed

prompt

delayed

prompt

400' coax in prompt   400' coax in delayed

$2 \times 8mm$ gap, $20\% \ CO_2$, $2.4 kV$, $0.2 \ V/div$

Figure 27

10. Two Track Resolution

An estimate of two track resolution was made by connecting two of

the chamber wires and putting a collimated [55]Fe source on one of them as

shown in Fig. 28 . Figure 29 shows the output of preamp A and (upper

trace) discriminator with the source in positions 1 and 2. The two

signals are of unequal height because the induced plulses of opposite

sign on the adjacent wires go only to one of the two. The resolution

distance increases by about 40 to 50% for preamp B which receives the

signals through nearly the full length of the delay line. Overall, the

two pulse resolution averages about 4 to 5 cm and ranges from 2.5 to 6.5

cm. Intermediate values are found when three wires are tied over to
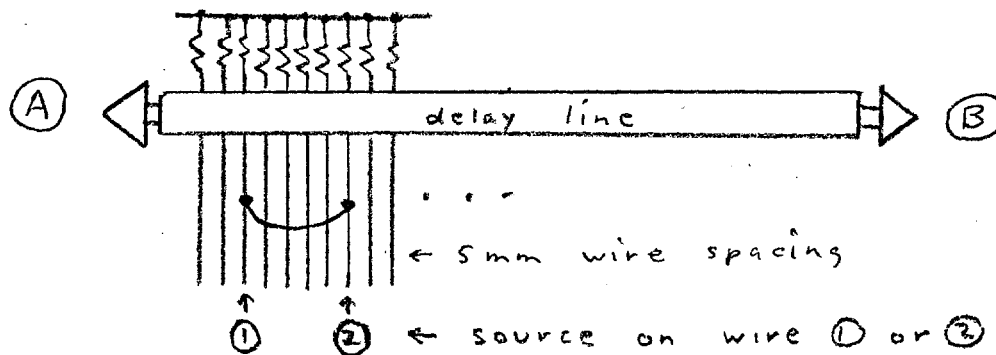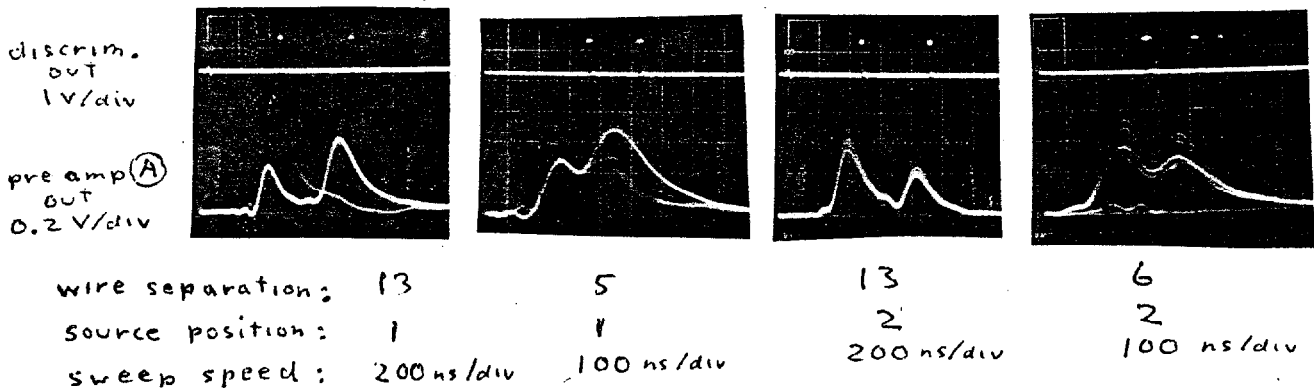
provide more nealy equal pulses.

Figure 28

discrim.
out
1 v/div

pre amp (A)
out
0.2 v/div

wire separation:	13	5	13	6
source position:	1	1	2	2
sweep speed :	200 ns/div	100 ns/div	200 ns/div	100 ns/div

2 x 8 mm gap, 2.4 kV, 20% CO_2 , 1 wire tied over

Figure 29

9. <u>High Voltage Circuit</u> – The high voltage circuit, shown in Figure 30 is

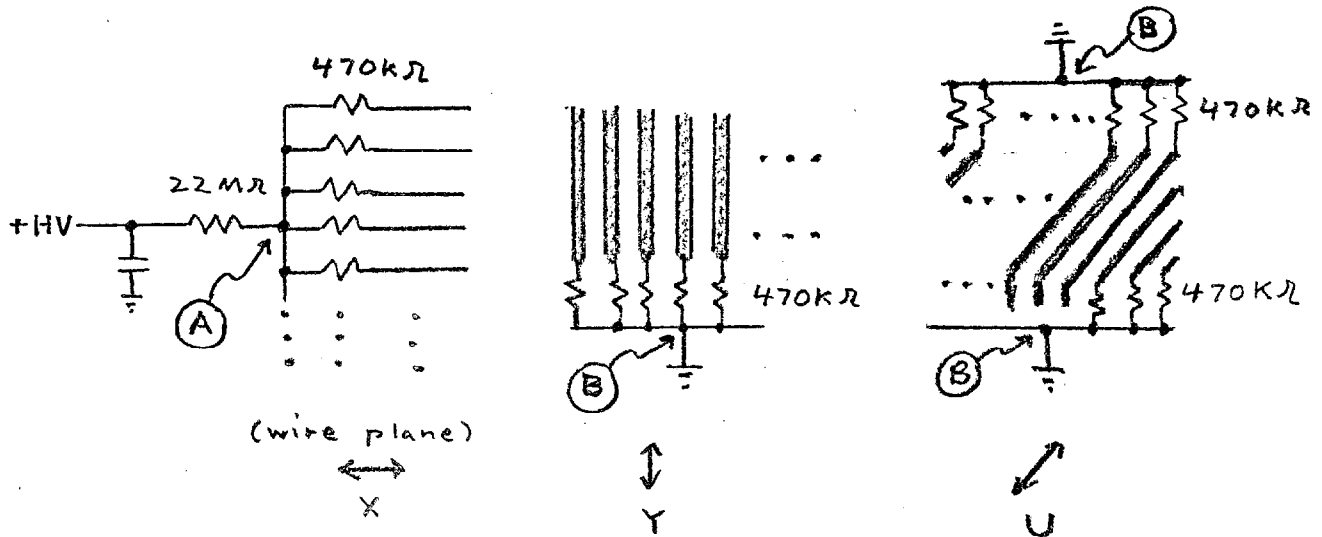essentially the same as that for the 12" chambers. The chamber has also

Figure 30

been run with point A tied to ground and points B brought to negative

high voltage to allow a direct measurement of the signal on the central

wires with a 1:1 probe. No difference in chamber operation was seen

(or expected). In the course of the testing, the chamber has survived

several disasters (turning the 1000 V knob instead of the 100 V knob

(SP), reversing polarity instead of changing voltage (RJ)···) with no

damage (except possibly to the experimenter's nerves). This is un-

doubtedly due to the 22 Meg Ω resistor which should be welded in in all

future installations. With chambers larger than the present one, the

chamber capacity becomes large enough to store a damaging amount of

energy (rule of thumb for 2kV and 20μ stainless steel wire: 10^2 pF

is OK, 10^3 pF is marginal, 10^4 pF is too much). Then the 470 K Ω

resistors will provide self isolation for the chamber as well as for the

delay lines.

REFERENCES

1. R. Grove, I. Ko, B. Leskovar and V. Perez-Mendez, Nucl. Instr. and Meth. 99, 381 (1972).

2. T. Trippe, Minimum Tension Requirement for Charpak Chamber Wires, CERN NP Internal Report 69-18 (1969).

3. Ray Fuzesy, Lawrence Berkeley Laboratory, (private communication).

4. S. Parker, R. Jones, J. Kadyk, M. L. Stevenson, T. Katsura, V. Z. Peterson, and D. Yount, Nucl. Instr. and Meth. 97, 181 (1971).

5. R. Muller, S. Derenzo, Lawrence Berkeley Laboratory, (private communication).